Large and Rapid Melt-Induced Velocity Changes in the Ablation Zone of the Greenland Ice Sheet

R. S. W. van de Wal, *et al.*

Science **321**, 111 (2008);
DOI: 10.1126/science.1158540

A detailed look at the AFM images of the first few monolayers reveals that the terrace height is not in agreement with the expected bulk value. The morphology of a nominally 1-nm-thick 6P film and the corresponding cross section through one of the islands are shown in Fig. 3, A and B. From these data, we deduce an island height of 2.05 nm ± 0.1 nm. Figure 3C shows the height histogram calculated from a 5-μm image of a 4-nm-thick 6P film. The peaks originate from the uncovered part of each terrace. We can calculate the average terrace height in the individual levels using Gaussians to fit the histogram. The height of the first three layers gradually increases toward the bulk value; cross sections through individual mounds (*16*) confirm this result. The change in terrace height can be explained by a varying tilt angle of the molecules in the first few layers. For the examined films, tilt angles (from the surface normal) between 43° (Fig. 3A) and 17° (bulk) are determined. The situation is sketched for the first four layers in Fig. 3D. Similar observations have already been made for copper phthalocyanine on highly ordered pyrolytic graphite (*29*).

Taking into account the larger tilt angles of the molecules in the first layers, we can calculate the transition state energy using the methods described above. The result of 0.23 eV is again in excellent agreement with the value determined from the analysis of the AFM images. Moreover, we can give a natural explanation for the reduced step-edge barrier. The molecular bending mechanism during interlayer mass transport results from the molecule needing to bend less in the case of the 43° tilted (001) surface. Thus, the required energy barrier for bending decreases, which leads to a rigorous lowering of the step-edge barrier. This effect is illustrated in Fig. 4A, where we plot the dependence of the ESB on the tilt angle of the (001) surface—the ESB depends on the growth stage. Figure 4B shows the bending energy as a function of the bending angle for an isolated molecule and illustrates the observed reduction of the ESB.

The sizable barrier height of 0.67 eV indicates that the growth of smooth films in a layer-by-layer manner is a challenging task for organic semiconductors. However, by carefully controlling the molecular orientation by surfactants or similar means, one might be able to reach that goal more easily than expected. The example of the rodlike 6P molecule shows that growth theories that are well known and verified in inorganic growth can also be used for organic growth. However, we have also demonstrated that the complex nature of the molecular building blocks leads to additional effects that are not observed in atomic inorganic growth.

References and Notes

1. C. K. Chiang *et al*., *Phys. Rev. Lett.* **39**, 1098 (1977).
2. E. Bauer, *Z. Kristallogr.* **110**, 372 (1958).
3. G. Ehrlich, F. Hudda, *J. Chem. Phys.* **44**, 1039 (1966).
4. R. L. Schwoebel, E. J. Shipsey, *J. Appl. Phys.* **37**, 3682 (1966).
5. M. Klaua, *Rost Krist.* **11**, 65 (1975).
6. K. Meinel, M. Klaua, H. Bethge, *J. Cryst. Growth* **89**, 447 (1988).
7. M. P. Seah, *Surf. Sci.* **32**, 703 (1972).
8. I. Elkinani, J. Villain, *Solid State Commun.* **87**, 105 (1993).
9. M. Kalff, P. Smilauer, G. Comsa, T. Michely, *Surf. Sci.* **426**, L447 (1999).
10. J. Krug, P. Politi, T. Michely, *Phys. Rev. B* **61**, 14037 (2000).
11. T. Michely, J. Krug, *Islands, Mounds and Atoms*, vol. 42 of Springer Series in Surface Science (Springer, Berlin, Heidelberg, 2004).
12. F.-J. Meyer zu Heringdorf, M. Reuter, R. Tromp, *Nature* **412**, 517 (2001).
13. L. Kilian, E. Umbach, M. Sokolowski, *Surf. Sci.* **573**, 359 (2004).
14. S. Zorba, Y. Shapir, Y. Gao, *Phys. Rev. B* **74**, 245410 (2006).
15. M. Fendrich, J. Krug, *Phys. Rev. B* **76**, 121302 (2007).
16. Details of the sample preparation, experiments, and calculations are available at *Science* Online.
17. H. Plank *et al*., *Thin Solid Films* **443**, 108 (2003).
18. F. Balzer, V. Bordo, A. Simonsen, H.-G. Rubahn, *Phys. Rev. B* **67**, 115408 (2003).
19. C. Teichert *et al*., *Appl. Phys. A* **82**, 665 (2006).
20. P. Frank *et al*., *Surf. Sci.* **601**, 2152 (2007).
21. R. Resel, *Thin Solid Films* **433**, 1 (2003).
22. Y.-P. Zhao, H.-N. Yang, G.-C. Wang, T.-M. Lu, *Phys. Rev. B* **57**, 1922 (1998).
23. J. Venables, G. Spiller, M. Hanbücken, *Rep. Prog. Phys.* **47**, 399 (1984).
24. P. Politi, *J. Phys. I* **7**, 797 (1997).
25. G. Koller, S. Surnev, M. Ramsey, F. Netzer, *Surf. Sci.* **559**, L187 (2004).
26. S. Schinzer, S. Köhler, G. Reents, *Eur. Phys. J. B* **15**, 161 (2000).
27. B. Yu, M. Scheffler, *Phys. Rev. B* **55**, 13916 (1997).
28. C. Teichert, C. Ammer, M. Klaua, *Phys. Status Solidi A Appl. Res.* **146**, 223 (1994).
29. H. Yamane *et al*., *J. Appl. Phys.* **99**, 093705 (2006).
30. D. W. Brenner *et al*., *J. Phys.* **14**, 783 (2002).

31. This project was supported by the Austrian Science Fund (FWF) Projects S9707, S9714, and P19197.

Supporting Online Material

www.sciencemag.org/cgi/content/full/321/5885/108/DC1
Materials and Methods
Figs. S1 to S3
References

22 April 2008; accepted 6 June 2008
10.1126/science.1159455

Large and Rapid Melt-Induced Velocity Changes in the Ablation Zone of the Greenland Ice Sheet

R. S. W. van de Wal,* W. Boot, M. R. van den Broeke, C. J. P. P. Smeets, C. H. Reijmer, J. J. A. Donker, J. Oerlemans

Continuous Global Positioning System observations reveal rapid and large ice velocity fluctuations in the western ablation zone of the Greenland Ice Sheet. Within days, ice velocity reacts to increased meltwater production and increases by a factor of 4. Such a response is much stronger and much faster than previously reported. Over a longer period of 17 years, annual ice velocities have decreased slightly, which suggests that the englacial hydraulic system adjusts constantly to the variable meltwater input, which results in a more or less constant ice flux over the years. The positive-feedback mechanism between melt rate and ice velocity appears to be a seasonal process that may have only a limited effect on the response of the ice sheet to climate warming over the next decades.

In the recent debate about the sensitivity of the Greenland Ice Sheet to climate warming, much attention has been given to increasing ice velocities. Widespread acceleration of outlet glaciers in southeast Greenland has been detected by satellite radar interferometry (*1*, *2*). These analyses focus on the discharge of outlet glaciers and indicate an increase of mass loss over the first few years of this century (*3*, *4*). Recent work on southeastern outlet glaciers indicates a decrease in the velocities to previous rates associated with a re-equilibration of the calving front (*5*); for Jakobshavn Isbrae along the west side, this is still unclear. In addition to the mass loss by calving, roughly 50% of the annual accumulation is lost by surface melting and runoff in the marginal areas of the ice sheet. Repeat-pass airborne laser altimetry suggests a slight thinning of the ice margin (*6*), although—at present—little ground validation of this finding exists. Concern about the dynamical stability of the ice sheet has also been raised by ground-based Global Positioning System (GPS) measurements at Swiss Camp (69.57°N, 49.31°W, 1175 m above sea level), indicating an additional ice displacement by increased summer velocities with a ratio up to 1.3 between summer and winter velocities (*7*). Clearly, we have to distinguish between mass loss via outlet glaciers and mass loss via increased ablation in the ice marginal zone. Both are affected by increased meltwater production, but the mechanics are different (*8*). On the ice sheet, these interferometry data, with 24-day temporal resolution, revealed summer speedups (50 to 100%) consistent with earlier observations (*7*) but smaller seasonal speedups where observed for outlet glaciers (<15%).

Here, we present ice velocity measurements from the major ablation area along the western margin of the ice sheet. The data set contains simultaneous measurements of ice velocity and ablation rates, which makes it possible to study the relation between ice velocity and meltwater input on longer (>5 years) and shorter (~1 day) time scales.

Institute for Marine and Atmospheric research Utrecht, Utrecht University, Netherlands.

*To whom correspondence should be addressed. E-mail: r.s.w.vandewal@uu.nl

The longest continuous time series of surface mass balance observations is that of the K-transect (Fig. 1), starting in 1991 (*9*). This record shows a large year-to-year variability, with ablation rates near the margin varying between 2.5 and 5.6 m of ice per year. The ablation rate in the area is significantly ($P < 0.05$, for linear trend) increasing over time (Fig. 2) but with a large interannual variability, whereas the position of the ice edge is unchanged. In addition to the surface mass balance measurements, stake positions have been recorded annually by GPS. These positions have been converted to annual ice velocities and are presented in Fig. 3A. Annual average ice velocities show a distinct spatial pattern, with the lowest velocities at the higher end of the transect, near Site 10, and the highest velocities at SHR, about 15 km from the ice front. More importantly, it can be observed that ice velocities decrease in time at some locations (Site 5, SHR, and Site 8) and are more or less constant for most other locations. The overall picture obtained by averaging all stake measurements at all sites for individual years indicates a small but significant ($r = 0.79$, $P < 0.05$) decrease of 10% in the annual average velocity over 17 years, which can possibly be attributed to a small decrease in the surface slope or ice thickness. Annually averaged velocities are completely decorrelated to the annual mass balance, whereas a correlation might be expected if there is a strong feedback between velocities and melt rate, leading to enhanced flow, surface lowering, and increased melt rates.

Against this background of slow changes over the past few years, we started more detailed position measurements in 2005 by taking advantage of technological developments of GPS equipment and data processing (*10*). The new instruments record hourly position of stakes, which are drilled into the ice. The GPS (single-frequency) units need to be serviced only once in a year and deliver an ice velocity record with a temporal resolution of 1 day or better.

Ice velocities for the 2005–06 melt season at the site SHR are shown in Fig. 3B. As soon as the surface melt starts in early May, ice velocities increase. Unexpectedly, substantial variations occur, which are superimposed on the gradual increase of the velocities over summer. Changes in ice velocity of up to 30% occur over weekly periods (Fig. 3B). This variability is much stronger than reported previously (*7*). Similar changes in velocity are observed along the entire transect (Fig. 3C). There is a coherent pattern over a distance of 60 km, although the largest changes are at SHR. Earlier in the season, the coherency is restricted to sites located close to each other.

At Sites 5, 6, and 9, automatic weather stations—which measure the ablation rate of the surface with a sonic height ranger—are operated. Combining these data with the high temporal velocity measurements reveals a rapid response of ice velocity to increased melt rates (Fig. 3D). Apparently, the increasing amount of meltwater from the surface penetrates to the base and leads to increased sliding velocities by raising the water pressure near the bed. The response is most prominent at SHR, because this site is located in a zone with many moulins. This finding points to a more general mechanism of meltwater penetration through the ice than the previously reported incidental drainage of a superglacial lake (*11*). Hitherto, the theoretical response of thick ice layers to meltwater fluctuations was assumed to be too slow to lead to weekly variations in the velocity of ice sheets, though observations (*7*) indicated a response. However, recent theoretical work (*12*) shows that if the formation of crevasses can be described by linear elastic fracture mechanics, response times are only of the order of weeks. Our measurements indicate that once the increased velocities are reached in summertime, velocity fluctuations may have an even shorter time scale. An explanation could be that crevasses only partly close during periods of decreased surface melting.

For alpine glaciers, it is known that ice velocities are higher in summer than in winter because of enhanced sliding (*13*, *14*). Local ice thickness on these glaciers is usually only a few hundred meters. Our observations demonstrate that in the ablation zone of the Greenland Ice Sheet, where ice thickness is 1000 to 1500 m, ice velocities respond to changes in the meltwater input within a week, which is in line with but more prominent than the responses observed in previous studies (*7*).

In earlier work (*4*, *7*), it has been suggested that the interaction between meltwater production and ice velocity provides a positive feedback, leading to a more rapid and stronger response of the ice sheet to climate warming than hitherto assumed. Our results are not quite in line with this view. We did not observe a correlation between annual ablation rate and annual ice velocities. Ice velocities respond fast to changes in ablation rate on a weekly time scale. However, on a longer time scale, the internal drainage system seems to adjust to the increased meltwater input in such a way that annual velocities remain fairly constant. In our view, the annual velocities in this part of the ice sheet respond slowly to changes in ice thickness and surface slope.

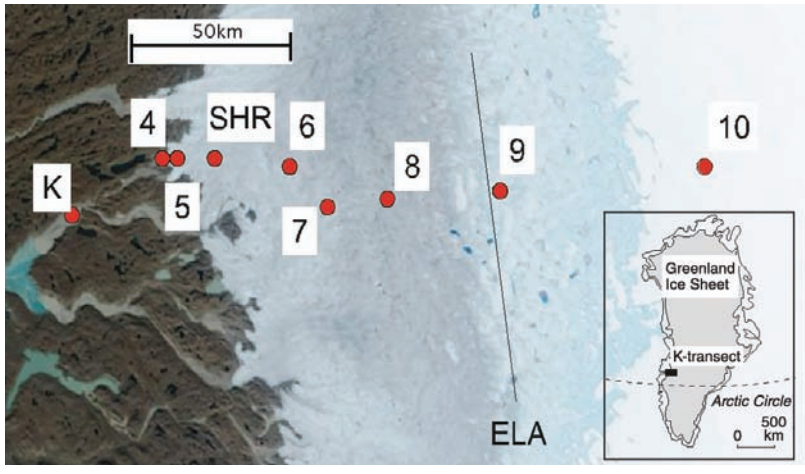

Fig. 1. The K-transect in west Greenland at 67°N. The background NASA–Modis/Terra image is dated 26 August 2003. K is Kangerlussuaq, whereas 4, 5, SHR, 6, 7, 8, and 9 are surface mass balance sites. ELA, Equilibrium Line Altitude. The equilibrium line (indicated by the black line) is at about 1500 m above sea level. The image clearly shows zones, from right to left, of snow (Site 10), wet snow (Site 9), dark ice (Site 8), and clear ice (Sites 4, 5, and SHR).

Fig. 2. The annual surface mass balance in the ablation zone of the K-transect averaged over five stations (Sites 4, 5, SHR, 6, and 9) with a continuous record over the past 17 years. Locations of the individual sites are shown in Fig. 1. "m. we," meter water equivalent.

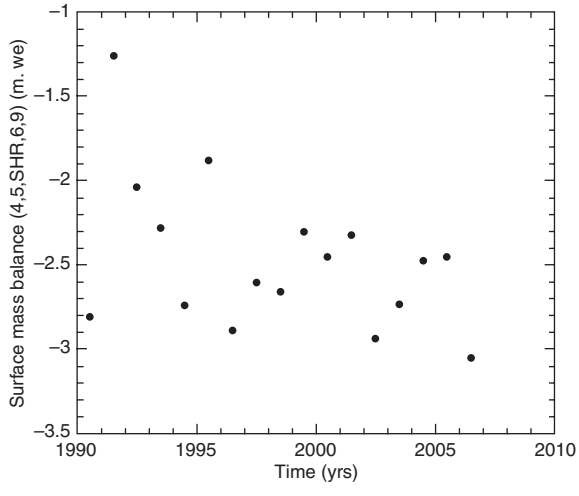

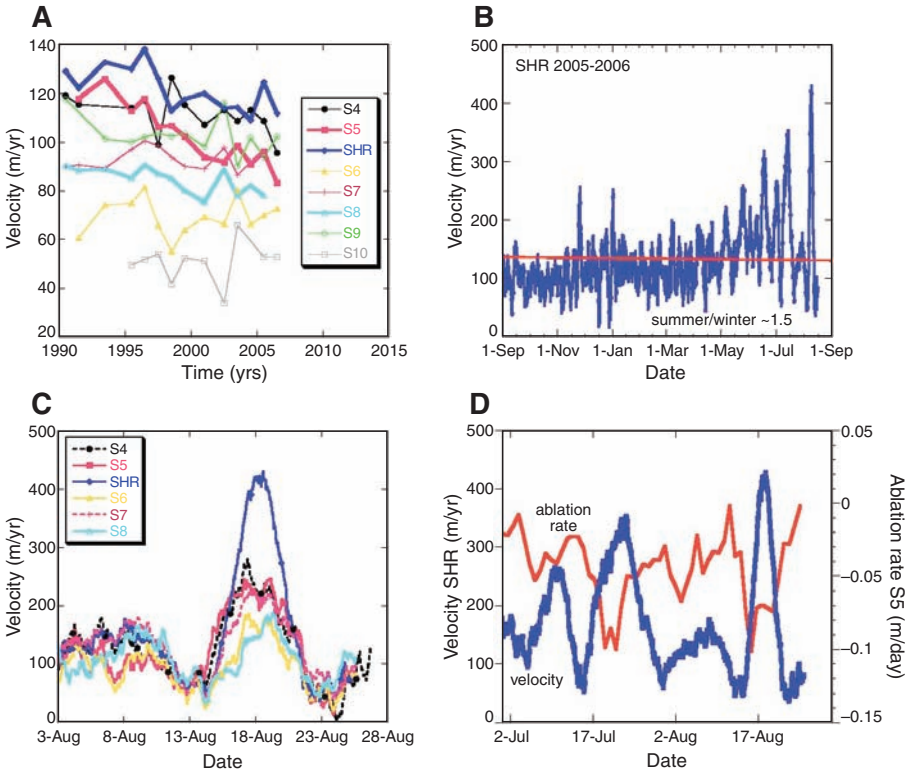

Fig. 3. (**A**) Variations in annual velocity along the K-transect over 17 years; sites with a significant decrease over time are depicted as thick lines. (**B** and **C**) Summer velocities at SHR are about 50% higher than winter velocities (B), which are in phase along the entire transect, particularly at the end of the melt season (C). (**D**) The changes in velocity are clearly related to the ablation rate. If the ablation rate increases, more meltwater is present and velocities increase; however, if ablation ceases, velocities decrease again. This implies that the change in meltwater, rather than the absolute amount of meltwater, determines the change of the velocity within a season.

Longer observational records with high temporal resolution in other ablation areas of the ice sheet are necessary to test the importance of the positive-feedback mechanism between melt rates and ice velocities. At present, we cannot conclude that this feedback is important. We do see a significant increase of the ablation rate (Fig. 2), which is likely related to climate warming, but it remains to be seen if this is likely to be amplified by increasing annual ice velocities.

References and Notes

1. W. Abdalati *et al.*, *J. Geophys. Res.* **106**, 33729 (2001).
2. E. Rignot, P. Kanagaratnam, *Science* **311**, 986 (2006).
3. L. A. Stearns, G. S. Hamilton, *Geophys. Res. Lett.* **34**, L05503 (2007).
4. P. Lemke *et al.*, in *Climate Change 2007*: *The Physical Science Basis. Contribution of Working Group 1 to the Fourth Assessment Report of the Intergovernmental Panel on Climate Change*, S. Solomon *et al.*, Eds. (Cambridge Univ. Press, Cambridge, 2007), pp. 337–383.
5. I. M. Howat, I. Joughin, T. A. Scambos, *Science* **315**, 1559 (2007).
6. W. B. Krabill *et al.*, *Geophys. Res. Lett.* **31**, L24402 (2004).
7. H. J. Zwally *et al.*, *Science* **297**, 218 (2002).
8. I. Joughin *et al.*, *Science* **320**, 781 (2008).
9. R. S. W. van de Wal, W. Greuell, M. R. van den Broeke, C. H. Reijmer, J. Oerlemans, *Ann. Glaciol.* **42**, 311 (2005).
10. T. Vincenty, *Surv. Rev.* **23**, 88 (1975).
11. S. B. Das *et al.*, *Science* **320**, 778 (2008).
12. C. J. van der Veen, *Geophys. Res. Lett.* **34**, L01501 (2007).
13. A. Iken, R. A. Bindschadler, *J. Glaciol.* **32**, 101 (1986).
14. T. C. Bartholomaus, R. A. Anderson, S. P. Anderson, *Nat. Geosci.* **1**, 33 (2008).

15. This work was supported by several grants from the Netherlands Organization of Scientific Research and the Netherlands Polar Programme.

1 April 2008; accepted 5 June 2008
10.1126/science.1158540

Mg/Al Ordering in Layered Double Hydroxides Revealed by Multinuclear NMR Spectroscopy

Paul J. Sideris,[1,2] Ulla Gro Nielsen,[1,2]* Zhehong Gan,[3] Clare P. Grey[1,2]†

The anion-exchange ability of layered double hydroxides (LDHs) has been exploited to create materials for use in catalysis, drug delivery, and environmental remediation. The specific cation arrangements in the hydroxide layers of hydrotalcite-like LDHs, of general formula $Mg^{2+}_{1-x}Al^{3+}_{x}OH_2(Anion^{n-}_{x/n})\cdot yH_2O$, have, however, remained elusive, and their elucidation could enhance the functional optimization of these materials. We applied rapid (60 kilohertz) magic angle spinning (MAS) to obtain high-resolution hydrogen-1 nuclear magnetic resonance (^{1}H NMR) spectra and characterize the magnesium and aluminum distribution. These data, in combination with ^{1}H-^{27}Al double-resonance and ^{25}Mg triple-quantum MAS NMR data, show that the cations are fully ordered for magnesium:aluminum ratios of 2:1 and that at lower aluminum content, a nonrandom distribution of cations persists, with no Al^{3+}-Al^{3+} close contacts. The application of rapid MAS NMR methods to investigate proton distributions in a wide range of materials is readily envisaged.

Hydrotalcite-like layered double hydroxides (LDHs) are a class of inorganic lamellar compounds with the general chemical composition $M^{2+}_{1-x}M^{3+}_{x}(OH)_2(A^{n-}_{x/n})\cdot yH_2O$, where M^{2+} and M^{3+} are divalent and typically trivalent metal cations respectively, x is the molar ratio of the trivalent cation $[M^{3+}/(M^{2+} + M^{3+})]$, which typically varies between 17% and 33% (*1*), and A^{n-} is an anion with charge n. The presence of a trivalent metal in the metal hydroxide $[M_{1-x}M'_x(OH)_2]$ sheet induces an overall positive charge, which is compensated by the incorporation of the anion, along with structural water, in the interlayer spaces (Fig. 1). One naturally occurring example of this class of materials is the mineral hydrotalcite, $Mg_6Al_2(OH)_{16}CO_3\cdot 4H_2O$, which contains carbonate ions in between the layers. The materials can accommodate a wide range of different anions (*2*) and cations (*3*), leading to a large compositional variety and thus tunability for a large number of applications.

These materials are of considerable geological relevance because of their anion-exchange capacity, which can affect the mobility of chemical species in the environment. Although there is a large group of materials with cation-exchange capabilities, the number of systems with positively charged frameworks or layers is extremely limited. LDHs are, therefore, attractive candidates as anion exchangers and can be used, for example, to remove toxic anions such as chromates (*4*), selenates (*5*), or halides (*6*) from waste waters or, more recently, as drug delivery systems (*7*). The materials are also frequently used as catalysts, catalyst supports, or precursors for oxides